Proc. Natl. Acad. Sci. USA
Vol. 82, pp. 1643–1647, March 1985
Biochemistry

Structure at 2.9-Å resolution of aspartate carbamoyltransferase complexed with the bisubstrate analogue *N*-(phosphonacetyl)-L-aspartate

(protein crystallography/enzyme activity/activity site)

KURT L. KRAUSE, KARL W. VOLZ, AND WILLIAM N. LIPSCOMB

Gibbs Chemical Laboratory, Harvard University, 12 Oxford Street, Cambridge, MA 02138

Contributed by William N. Lipscomb, November 13, 1984

ABSTRACT **In an x-ray diffraction study by the isomorphous replacement method, the structure of the complex of aspartate carbamoyltransferase (EC 2.1.3.2) bound to the bisubstrate analogue *N*-(phosphonacetyl)-L-aspartate has been solved to 2.9-Å resolution (R = 0.24). The large quaternary structural changes previously deduced by molecular replacement methods have been confirmed: the two catalytic trimers (c_3) move apart by 12 Å and mutually reorient by 10°, and the regulatory dimers (r_2) reorient each about its twofold axis by about 15°. In this, the T-to-R transition, new polar interactions develop between equatorial domains of c chains and the Zn domain of r chains. Within the c chain the two domains, one binding the phosphonate moiety (polar) and the other binding the aspartate moiety (equatorial) of the inhibitor *N*-(phosphonacetyl)-L-aspartate, move closer together. The Lys-84 loop makes a large relocation so that this residue and Ser-80 bind to the inhibitor of an adjacent catalytic chain within c_3. A very large change in tertiary structure brings the 230–245 loop nearer the active site, allowing Arg-229 and Gln-231 to bind to the inhibitor. His-134 is close to the carbonyl group of the inhibitor, and Ser-52 is adjacent to its phosphonate group. However, no evidence exists in the literature for phosphorylation of serine in the mechanism. Residues studied by other methods, including Cys-47, Tyr-165, Lys-232, and Tyr-240, are too far from the inhibitor to have a direct interaction.**

Aspartate carbamoyltransferase (carbamoyl phosphate:L-aspartate carbamoyltransferase, EC 2.1.3.2) of *Escherichia coli* is an allosteric enzyme that begins pyrimidine biosynthesis by synthesizing carbamoyl-L-aspartate from L-aspartate and carbamoyl phosphate. Homotropic cooperativity is induced by both substrates (1, 2), and heterotropic effects involve inhibition by CTP and activation by ATP (1, 3). The structure consists of catalytic (c) and regulatory (r) chains in a $(c_3)_2(r_2)_3$ oligomer which has D_3 symmetry (Fig. 1) (4–6). Previous x-ray diffraction studies have established the structure of the less active T form to a resolution of 2.6 Å (7, 8). Also, the large changes in quaternary structure that occur in the transition to the R form as the bisubstrate analogue *N*-(phosphonacetyl)-L-aspartate (PALA) is bound have been described (9). Less precise indications of these large conformational changes have been established by other investigators (10–13). Our refinement of this R form proceeded so slowly that we have undertaken an independent solution of the R structure bound to PALA by the method of multiple isomorphous replacement (MIR). The results, described below, establish the binding site of PALA and elucidate previously undescribed changes in tertiary structure of the catalytic chains, and they also enable us to look at the T-to-R homotropic transition as typified by these two x-ray structures: unligated- and PALA-aspartate carbamoyltransferase.

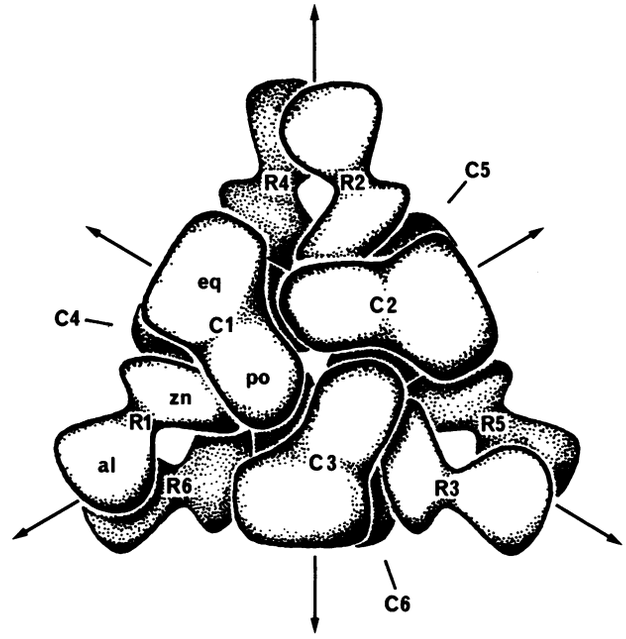

FIG. 1. Subunit and domain structure of aspartate carbamoyltransferase, as viewed down the threefold axis. Domains of the catalytic (c) chains C1–C6 are equatorial (eq) and polar (po), while those of the regulatory (r) chains R1–R6 are zinc (zn) and allosteric (al).

MATERIALS AND METHODS

Crystal Growth. The enzyme was isolated and purified (14) from regulatory mutant *E. coli* provided by J. C. Gerhart and grown at the New England Enzyme Center. Crystals were obtained by dialyzing for 1–2 weeks at 21°C against 50 mM maleic acid/1 mM PALA/3 mM NaN_3/*N*-ethylmorpholine to pH 5.9 and conductivity 3.4 mS. Temperature control was critical for crystallization. After growth, the crystals were transferred, still within their microdialysis vials, to 20% (wt/vol) polyethylene glycol-6000/crystallization buffer at pH 5.8. The crystals were hexagonal bars, in the space group $P321$, and unit cell dimensions are $a = b = 122.1$ Å and $c = 156.2$ Å. There are two rc units related by an approximate noncrystallographic twofold axis in the unit cell. Heavy atom derivatives were made by transferring crystals to

The publication costs of this article were defrayed in part by page charge payment. This article must therefore be hereby marked "*advertisement*" in accordance with 18 U.S.C. §1734 solely to indicate this fact.

Abbreviations: PALA, *N*-(phosphonacetyl)-L-aspartate; c, catalytic subunit; r, regulatory subunit; MIR, multiple isomorphous replacement.

similarly buffered solutions containing also either 1 mM $K_2Pt(NO_2)_4$ (4–7 days) or 5.6 mM K_3IrCl_6 (3 days).

Data and Analysis. The final data sets were collected in the laboratory of Nguyen huu Xuong at the University of California, San Diego, using two multiwire proportional chambers (MARK II) (15) and an Elliot GX-6 rotating anode unit (40 kV and 50 mA). The x-rays were monochromatized, and the Nicolet goniostat was driven by a VAX 11/750 computer. We chose crystals of typical dimensions 0.7 × 0.7 × 1.2 mm and mounted them in silane-treated glass capillaries, which were then sealed. The native protein data set, containing 415,000 observations of 51,000 independent reflections, is 97% complete to 2.5 Å. The data set for the $K_2Pt(NO_2)_4$ derivative contains 330,000 observations of 42,000 reflections and is essentially complete to 2.7 Å. Some 95,000 observations of 22,000 reflections were collected for the K_3IrCl_6 derivative which is, therefore, complete to 3.4 Å. Using programs developed at San Diego, we scaled the observations in 5° increments of ω, averaged, and applied Lorentz-polarization corrections. After critiquing, we found R_{sym} values of 6.1%, 5.8%, and 4.7% for the native, $K_2Pt(NO_2)_4$, and K_3IrCl_6 data sets, respectively.

Structure Refinement. Phases from the molecular replacement study were used in conjunction with Patterson maps to locate the heavy atom sites. Locations, occupancies, and temperature factors of these sites were refined by using either centroid or most probable phases (16). Final electron density maps were calculated by using centroid phases. For real space averaging, an initial location of the noncrystallographic twofold axis was obtained from the heavy atom positions by least-squares procedures. This location was refined in real space by the method of Cox (17) separately for each of the four structural domains: polar, equatorial, zinc, and allosteric (Fig. 1). Excluding the allosteric domain (see below), we weighted the remaining three locations by their correlation coefficients and combined them into the twofold axis for use in the averaging process. Real-space averaging of the electron density obtained by MIR methods was then carried out by using programs of Bricogne (18, 19). Convergence to an *R*-factor of 0.20 was obtained after four cycles, and the resulting phases were used to calculate $2F_o - F_c$ and $F_o - F_c$ maps, F_o and F_c being observed and calculated amplitudes, respectively.

Building of the structure into these maps was carried out on either an Evans and Sutherland MPSII or PS300 system interfaced to a VAX 11/780. The graphics software was developed by Diamond (20) as modified by R. Ladner (BILDER) or written by Jones (21) as modified by Pflugrath and Saper (FRODO). After the model was manipulated into density it was refined by using the reciprocal-space-restrained least-squares method of Hendrickson and Konnert (22). Conjugant gradient calculations were made by the method of Jack (23). No noncrystallographic symmetry was used in the restraints. So far, 88 cycles of reciprocal space refinement and 8 rebuilding sessions have yielded a crystallographic *R* value of 0.24 for the 32,000 unique reflections to 2.9-Å resolution. Root-mean-square deviations of the observed bond distances and angles from ideality have been restrained to 0.021 Å and 4.3°, respectively.

RESULTS

A total of 92% of protein sequence has been built into electron density. The connectivity of the polypeptide chains is the same as in our earlier studies. In each c chain the course of the polypeptide is clear except for residues 308–310, although ambiguities of positions occur for several chains. In each r chain areas of excellent density occur in the zinc domain and in the five strands of β-sheet of an allosteric domain, but about 25 residues occur without density (1–15 and 50–60). On the basis of those aspects of the structure that appear unambiguous at this stage of refinement, we offer the following conclusions.

The quaternary structural changes described previously (9) have been confirmed. As the T-to-R transformation occurs, the two catalytic trimers become mutually reoriented by 10° relative to one another, adopting a more eclipsed position; i.e., one c_3 reorients by 5° while the other reorients by −5° (Fig. 2). Second, each regulatory dimer reorients by 15° around its twofold axis. Third, the entire complex elongates by 12 Å along the molecular threefold axis—i.e., one c_3 moves 6 Å while the other moves −6 Å (Fig. 2). Fourth, and not previously described, the equatorial domains of the c chains relocate about 3 Å closer to the phosphate site, defined here as the pyrophosphate site of the T form and the similarly located phosphonate site of PALA in the R form of the enzyme, as described below. This shift, shown in Fig. 3, allows increased interactions at the C1–R1 (equatorial domain) interface but preserves the C1–R1 (polar domain) interactions previously reported for the T state (7, 8).

An apparent small structural change reduces the molecular symmetry from D_3 to C_3. The twofold axes for the polar, equatorial, zinc, and allosteric domains are 12.2°, 12.9°, 11.6°, and 9.9°, respectively, away from the crystallographic *y* axis (corresponding correlation coefficients are 0.56, 0.53, 0.51, and 0.40). While the orientation of the allosteric domain appears to be significantly different from the average for the other three domains, this result must be considered tentative because it is based on the MIR density and not on final coordinates. It is unclear whether this small deviation is a property of the isolated molecule or, perhaps more likely, of the molecular packing in the crystal.

The tertiary structural changes in the catalytic chains are large in the 80s loop and the 240s loop (Fig. 3). A movement of 5 Å in the 80s loop brings Ser-80 and Lys-84 near the phosphonate of PALA in an adjacent c chain of a catalytic trimer. The repositioning of the 240s loop brings it much nearer the PALA molecule, but the effect is a completely altered C1–C4 interface, which results from a combination of this repositioning and the associated mutual reorientation of the catalytic trimers (Fig. 2). For example, Asp-236 to Tyr-240 are side by side in the T form but are opposite one another in the R form of the enzyme. Indeed, this contact (238–240) is the only direct C1···C4 interaction in the R form. The bonding interactions, respectively, of Lys-164 and Tyr-165 to Asp-236 and Glu-239 of the opposite (other c_3) catalytic chain in the T form no longer exist in the R form, and the C1–R4 interactions are no longer present. Instead, new contacts exist between Glu-239 and residues 164 and 165, all within the same c chain.

The PALA molecule is located near the amino terminus (residues 52–55) of the second α-helix of the polar domain. Its phosphonate group is at the previously reported pyrophosphate site of the T state (24). The phosphonate and carboxylate groups of PALA protrude from the *si* face of the prochiral carbonyl group in a configuration somewhat different from that in the crystal structure of PALA (25). A dihedral angle of about 110° occurs between the carboxylate groups, when viewed along the α–β bond of C—C_α—C_β—C_γ.

Charged residues in the chamber surrounding PALA (Fig. 4) include Glu-50, Arg-54, Arg-105, Arg-167, Arg-229, Glu-233, Arg-234, and Arg-296 from one c chain, and also Lys-84 and Lys-83 from an adjacent c chain of the c_3 subunit. This chamber is accessible only from the central cavity. The new position of the 240s loop in the R form forms a lower boundary to this chamber. In this region, new bonds between the equatorial domain and the polar domain include

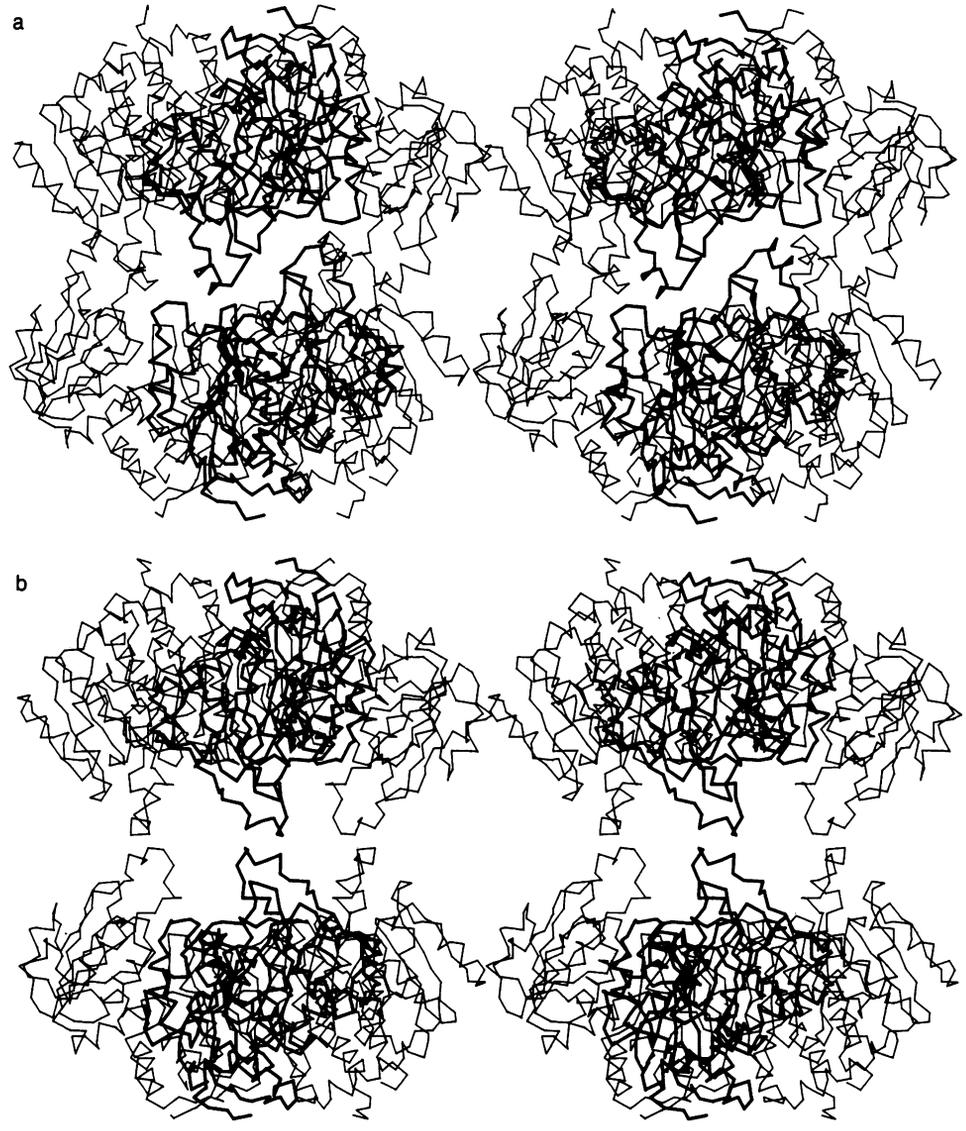

FIG. 2. The polypeptide chains of the two catalytic trimers in the less active (T) conformation (*a*) and in the more active (R) conformation (*b*). The r chains have been omitted for clarity. In this figure the view is from the side of the molecule perpendicular to the threefold axis, which now lies in the plane of the paper in the vertical direction.

those between Glu-50 and Arg-167 and between Glu-50 and Arg-234.

Within the active site PALA interacts as follows. The phosphonate group is near Ser-52, Arg-54, Thr-55, Arg-105 of one c chain, and Ser-80 and Lys-84 of the adjacent c chain. (Arg-54 also has a major interaction in a salt bridge to Glu-86 of the adjacent c chain.) The α-carboxylate is near Arg-105 and Arg-167 and is also near (adjacent chain) Lys-84. The β-carboxylate is nearest to Arg-229 and Gln-231 and is not far from Thr-168. Near the carbonyl oxygen of the peptide group in PALA we find His-134. The amide NH of this peptide group is near the backbone carbonyl oxygen of Leu-267.

DISCUSSION

Aspartate carbamoyltransferase is an important example of an allosteric enzyme for which structures are known for both T and R forms. The binding of PALA stabilizes an R state that is dramatically different from the T state of the enzyme. The gross conformational changes, which involve large-scale repositioning of the subunits, leave some interface interactions constant but cause substantial restructuring of almost all interfaces between domains. The accompanying tertiary and local structural rearrangements cause a major reconstruction of the active site. We comment on some of these changes.

The quaternary changes in structure are consistent with those reported previously from this laboratory (9). However, the changes in tertiary structure have not been reported previously: the largest, in the 240s loop (225–245), causes the upper c_3 to stack against the lower c_3, and thus it helps to prevent collapse of the R form to the T form along the direction of the threefold axis. New salt bridges form between the equatorial and polar domains as well as with PALA to aid in maintaining the R conformation. The repositioning of Glu-228, Arg-229, Gln-231, and Arg-234 into each active site is linked to the change of Glu-239 from inter- to intrasubunit bonding to Lys-164 and Tyr-165 as T goes to R. This trimer–trimer interface may provide one pathway for homotropic interactions.

The second largest change in tertiary structure of the c chain brings Ser-80 and Lys-84 of an adjacent c chain into the active site. This result confirms our earlier suggestion of an active site shared between adjacent c chains within c_3 subunits (26).

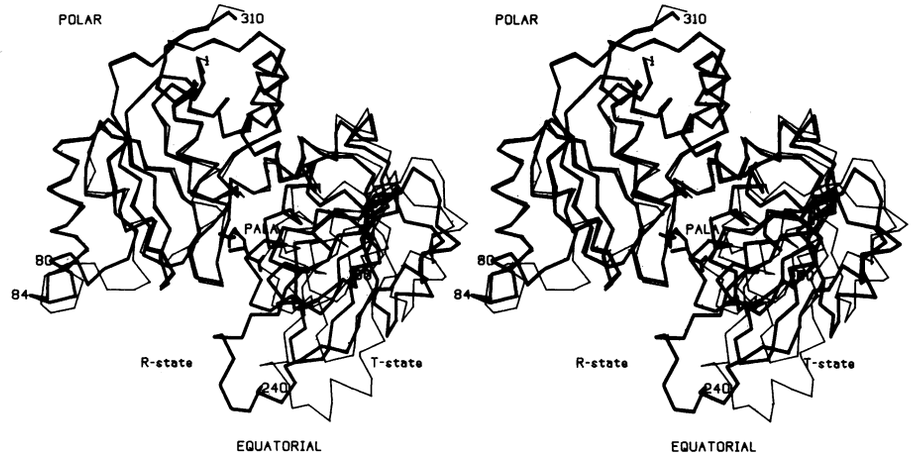

FIG. 3. Superposition of the c chain of the T (thin line) and R (thick line) conformations. We have chosen to superimpose most closely the polar domains. The view is perpendicular to the threefold axis. The location of the PALA molecules in the R state is shown. Large changes in conformation occur near Tyr-240 and more modest changes occur in the region near Lys-84. New bonds form between both Arg-167 and Arg-234 of the equatorial domain to Glu-50 of the polar domain in the T-to-R transition.

The PALA molecule is bound by many interactions, including electrostatic and hydrogen bonding contacts as described in the previous sections, and possibly the negative end of the dipole of the second α-helix of the c chain. Binding of this phosphonate group to the R form is similar to the binding of pyrophosphate to the T form except that Lys-84 does not bind to pyrophosphate and Arg-54 maintains, as in the unligated structure, another major interaction, with Glu-86, in the R form. No direct interaction occurs between Lys-83 and PALA, although this lysine is nearby. The relationship of these lysines, including also Lys-232, to the activity has been studied by chemical modification (11, 27). A Ser-52 mutation (28) to Phe-52 inactivates the enzyme, probably because the bulky phenyl group would interfere with the binding of the PALA's phosphonate group, which is close to Ser-52 in the structure. The Gly-128 to Asp mutation (29, 30) introduces a negative charge into a critical region of positive charges. Other residues implicated by chemical modification or mutagenesis are Cys-47 (31, 32), Tyr-165 (33), Lys-232 (27), and Tyr-240 (34). None of these is close enough to PALA to be involved in binding. For example, Tyr-165, found to be 17 Å away from the pyrophosphate site of the T form in our earlier study, is also about 17 Å away from the phosphonate site in the R form. There is no density to support relocation of Tyr-165 by a 180° rotation about the α–β bond, although such a rotation, coupled with displacement of Gln-231, could bring Tyr-165 close to the PALA molecule. A very recent mutagenesis study indicates that some activity is retained when Tyr-165 is modified (35).

One or more histidine residues have been implicated in possible general acid catalysis of the nucleophilic attack of the amino group of L-aspartate on carbamoyl phosphate (24, 36). In our structure His-134, near the carbonyl group of PALA, is the only potentially catalytic side chain in this region, assuming that Ser-52 and Ser-80 are involved only in binding.

There are many positively charged residues in and near

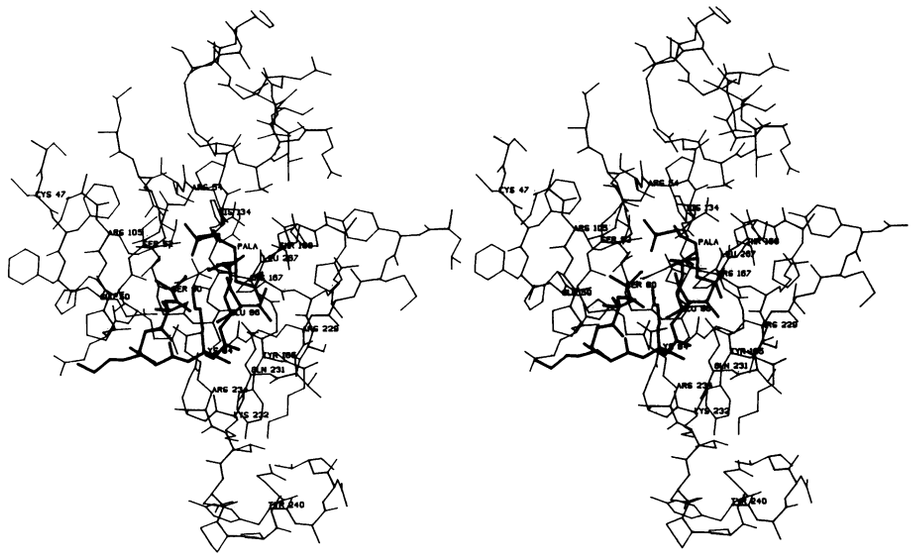

FIG. 4. Detailed structure shown around the binding site for PALA as viewed from the central cavity of the enzyme, perpendicular to the threefold axis. The PALA molecule plus residues 80–87 from the adjacent chain are drawn with a thick line, while the c chain most closely associated with the PALA molecule is drawn with thin lines. His-134, near the carbonyl oxygen of PALA, is between the polar domain (smaller numbers), which dominates binding of the phosphonate moiety, and the equatorial domain (larger numbers), which predominately binds the aspartate moiety of PALA. Some of the other interactions and residues far from PALA such as Cys-47, Tyr-165, and Tyr-240 are discussed in the text.

the binding site of PALA. It remains to be shown that other small phosphates, such as analogues of carbamoyl phosphate, bind in this region. Indeed, there are indications that at least one other nearby binding site for anions is present, in view of the kinetic studies of Heyde (37), and the substantial substrate inhibition by aspartate (38). Structural studies are needed of simultaneous binding of aspartate or succinate to the PALA enzyme.

In summary, we see that the negative charges of the PALA molecule promote changes in tertiary structure of the catalytic chains. Lys-84 is drawn into the active site from an adjacent catalytic chain. Within the same catalytic chain the large movement of the 240s loop, facilitated by binding of Arg-229 and Gln-231 to PALA, occurs when the catalytic trimers move apart and reorient about the molecular threefold axis. Preservation of the crrc units requires reorientation of the regulatory dimer. The many other changes in interactions that occur in the allosteric transition will be described in a future publication following further refinement of the structure.

We thank R. Hubbard and D. States for the programs HYDRA and PLT2, respectively, which were used to prepare the figures, and we thank J. Ladner and R. Ladner for help and advice. The diffraction data were collected at the Resource for Crystallography at the University of California, San Diego, funded by Grant RR01644 to N. h. Xuong. We thank him, R. Hamlin, and C. Nielson for aid in the use of this facility. This research was supported by Grant GMO6920 from the National Institutes of Health.

1. Gerhart, J. C. & Pardee, A. B. (1962) *J. Biol. Chem.* **237,** 891–896.
2. Bethell, M. R., Smith, K. E., White, J. S. & Jones, M. E. (1968) *Proc. Natl. Acad. Sci. USA* **60,** 1442–1449.
3. Gerhart, J. C. & Pardee, A. B. (1964) *Fed. Proc. Fed. Am. Soc. Exp. Biol.* **23,** 727–735.
4. Weber, K. (1968) *Nature (London)* **218,** 1116–1119.
5. Wiley, D. C. & Lipscomb, W. N. (1968) *Nature (London)* **218,** 1119–1121.
6. Wiley, D. C., Evans, D. R., Warren, S. G., MacMurray, C. H., Edwards, B. F. P., Franks, W. A. & Lipscomb, W. N. (1972) *Cold Spring Harbor Symp. Quant. Biol.* **36,** 285–290.
7. Honzatko, R. B., Crawford, J. L., Monaco, H. L., Ladner, J. E., Edwards, B. F. P., Evans, D. R., Warren, S. G., Wiley, D. C., Ladner, R. C. & Lipscomb, W. N. (1982) *J. Mol. Biol.* **160,** 219–263.
8. Ke, H. M., Honzatko, R. B. & Lipscomb, W. N. (1984) *Proc. Natl. Acad. Sci. USA* **81,** 4037–4040.
9. Ladner, J. E., Kitchell, J. P., Honzatko, R. B., Ke, H. M., Volz, K. W., Kalb (Gilboa), A. J., Ladner, R. C. & Lipscomb, W. N. (1982) *Proc. Natl. Acad. Sci. USA* **79,** 3125–3128.
10. Collins, K. D. & Stark, G. R. (1971) *J. Biol. Chem.* **246,** 6599–6605.
11. Kempe, T. D. & Stark, G. R. (1975) *J. Biol. Chem.* **250,** 6861–6869.
12. Howlett, G. J. & Schachman, H. K. (1977) *Biochemistry* **16,** 5077–5083.
13. Moody, M. F., Vachette, P. & Foote, A. M. (1979) *J. Mol. Biol.* **133,** 517–532.
14. Gerhart, J. C. & Holoubek, H. (1967) *J. Biol. Chem.* **242,** 2886–2892.
15. Hamlin, R., Cork, C., Howard, A., Nielsen, C., Vernon, W., Matthews, D. & Xuong, N. h. (1981) *J. Appl. Crystallogr.* **14,** 85–93.
16. Blow, D. M. & Crick, F. H. C. (1959) *Acta Crystallogr.* **12,** 794–802.
17. Cox, J. M. (1967) *J. Mol. Biol.* **28,** 151–156.
18. Bricogne, G. (1974) *Acta Crystallogr. Sect. A* **30,** 395–405.
19. Bricogne, G. (1976) *Acta Crystallogr. Sect. A* **32,** 832–847.
20. Diamond, R. (1982) in *Computational Crystallography*, ed. Sayre, D. (Oxford, London), pp. 318–325.
21. Jones, T. A. (1982) in *Computational Crystallography*, ed. Sayre, D. (Oxford, London), pp. 303–317.
22. Hendrickson, W. A. & Konnert, J. (1981) in *Biomolecular Structure, Function, and Evolution*, ed. Srinivasan, R. (Pergamon, London), Vol. 1, pp. 43–47.
23. Jack, A. & Levitt, M. (1978) *Acta Crystallogr. Sect. A* **34,** 931–935.
24. Honzatko, R. B. & Lipscomb, W. N. (1982) *J. Mol. Biol.* **160,** 265–286.
25. Zanotti, G., Monaco, H. L. & Foote, J. (1984) *J. Am. Chem. Soc.* **106,** 7900–7904.
26. Monaco, H. L., Crawford, J. L. & Lipscomb, W. N. (1978) *Proc. Natl. Acad. Sci. USA* **75,** 5276–5280.
27. Lauritzen, A. M. & Lipscomb, W. N. (1982) *J. Biol. Chem.* **257,** 1312–1319.
28. Schachman, H. K., Pauza, C. D., Navre, M., Karels, M. J., Wu, L. & Yang, Y. R. (1984) *Proc. Natl. Acad. Sci. USA* **81,** 115–119.
29. Wall, K. A., Flatgaard, J. E., Gibbons, I. & Schachman, H. K. (1979) *J. Biol. Chem.* **254,** 11910–11916.
30. Wall, K. A. & Schachman, H. K. (1979) *J. Biol. Chem.* **254,** 11917–11926.
31. Evans, D. R. & Lipscomb, W. N. (1979) *J. Biol. Chem.* **254,** 10679–10685.
32. Vanaman, T. C. & Stark, G. R. (1970) *J. Biol. Chem.* **245,** 3565–3573.
33. Lauritzen, A. M., Landfear, S. M. & Lipscomb, W. N. (1980) *J. Biol. Chem.* **255,** 602–607.
34. Landfear, S. M., Evans, D. R. & Lipscomb, W. N. (1978) *Proc. Natl. Acad. Sci. USA* **75,** 2654–2658.
35. Robey, E. A. & Schachman, H. K. (1984) *J. Biol. Chem.* **259,** 1180–1183.
36. Greenwell, P., Jewett, S. L. & Stark, G. R. (1973) *J. Biol. Chem.* **248,** 5994–6001.
37. Heyde, E. (1976) *Biochim. Biophys. Acta* **452,** 81–88.
38. Pastra-Landis, S. C., Evans, D. R. & Lipscomb, W. N. (1978) *J. Biol. Chem.* **253,** 4624–4630.